

# Broadband Stationary Fourier Transform Spectrometer Integrated on a Silicon Nitride Photonics Platform

Xiaomin Nie<sup>1,2</sup>, Eva Ryckeboer<sup>1,2</sup>, Gunther Roelkens<sup>1,2</sup> and Roel Baets<sup>1,2</sup>

<sup>1</sup> Photonics Research Group, Department of Information Technology, Ghent University-imec, Ghent B-9000, Belgium

<sup>2</sup> Center for Nano- and Biophotonics(NB-Photonics), Ghent University, Ghent B-9000, Belgium

e-mail: Xiaomin.Nie@ugent.be

**Abstract:** We experimentally demonstrate a novel type of Fourier transform spectrometer that is integrated on a  $Si_3N_4$  waveguide platform. It features an extremely small size ( $0.1 \text{ mm}^2$ ) with high resolution (6 nm) and large bandwidth ( $>100 \text{ nm}$ ).

**OCIS codes:** (130.3120) Integrated optics devices, (300.6190) Spectrometers.

## 1. Introduction

In recent years a lot of research efforts are targeted at the miniaturization of Fourier Transform Spectrometers (FTS). Small and robust spectrometers offer the advantage of portability. An extremely small FTS can be realized using Silicon photonics technology. This technology uses CMOS compatible processes to integrate a complete spectrometer on a semi-conductor chip. This chip is robust and can be cheaply fabricated in large quantities. Integrated Fourier Transform Spectrometers can be divided into two categories: a Stationary Wave Integrated FTS (SWIFTs) [1] and the Spatial Heterodyne Spectrometer (SHS) [2]. In both cases, the generated interferogram is a spatial field distribution that is captured with a photodiode array. In an integrated SHS, a large set of Mach-Zehnder interferometers (MZI) is used. Each MZI creates a section of the Fourier interferogram. Therefore, a large SHS is needed for long interferogram which leads to high resolution. For SWIFTs, a high resolution can be achieved in a small footprint. The basic principle of operation is the interference of two beams which creates a standing wave pattern (the interferogram) inside a single waveguide. This standing wave pattern is then coupled from the waveguide to a detector array using nano-scatterers. The periods that are present in the interferogram  $\lambda/(2n_{eff})$  are much smaller than the pitch of state-of-the-art photodiode arrays and therefore the interferogram is subsampled. This limits the spectral bandwidth of the FTS. To overcome this problem, we propose a new stationary wave integrated FTS design. This design lifts the bandwidth restriction by creating a stretched interferogram in between two waveguides. Here we will discuss the theory, simulation results and first experimental results of this novel FTS. The prototype FTS was fabricated on a  $Si_3N_4$  waveguide platform and evaluated with a narrowband light source. The measurements show good correspondence with the expected performance.

## 2. Design of the Co-propagative Stationary FTS

The stationary FTS we propose relies on the interference between two different co-propagative waveguide modes, and is thus called co-propagative stationary FTS. As depicted in the schematic drawing (Fig. 1(a)), the signal to be analyzed is injected and split into two parallel waveguides with a different width by a 3dB Multimode Interference coupler (MMI). Since the two excited waveguide modes have different propagation indices, they will have different phase delays after propagating the same distance. Their evanescent tails will slightly overlap and interfere with each other as we properly space the two parallel waveguides. To probe the generated interferogram, we place a well-designed grating in between the two waveguides. With the proper grating period, the interference pattern can be diffracted upwards onto the detector array positioned in the near field. Assuming a signal at a wavelength  $\lambda$ , the intensity of the interferogram will vary as  $\cos(\Delta\beta z)$ , where  $\Delta\beta = \beta_1 - \beta_2$  is the difference in propagation indices of the two waveguide modes considered and  $z$  is the propagation distance. One can further write  $\Delta\beta$  as  $2\pi\Delta n_{eff}/\lambda$  with  $\Delta n_{eff}$  the difference in effective index of the two waveguide modes. Therefore, the period of the interferogram can be expressed as  $\lambda/\Delta n_{eff}$  which is improved by a factor of  $2n_{eff}/\Delta n_{eff}$  when compared to the original SWIFTs design [1]. As a result, one can easily find commercially available photodiode arrays with pixel pitch small enough to avoid subsampling of the interferogram.

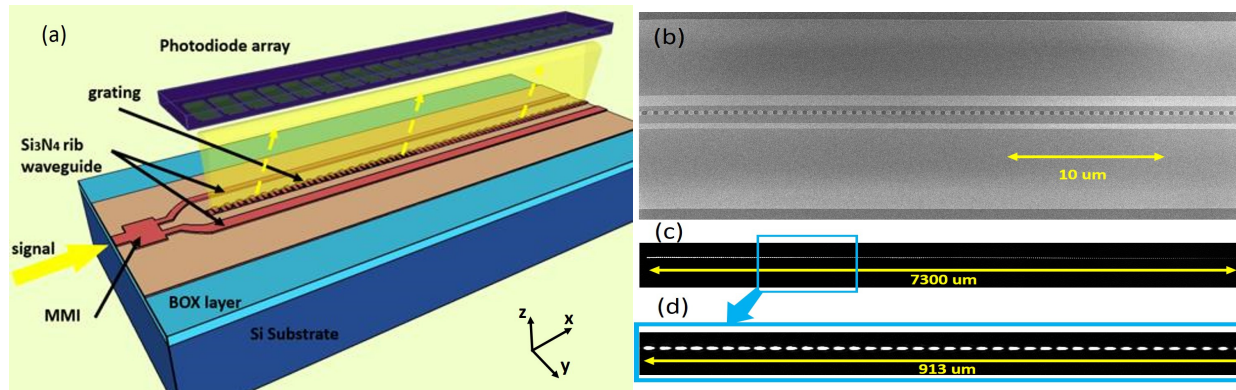


Fig. 1: (a) Conceptual drawing of the co-propagative stationary FTS [4] (b) SEM picture of a small part of the fabricated co-propagative stationary FTS (c) the optical view of the full interferogram (d) a zoom-in of the interferogram in the blue box in (c) .

The most important component in the co-propagative stationary FTS is the grating. The design of the grating should aim at a strong directionality and a very weak reflection. The former allows the grating to diffract most of the optical power upwards while the latter helps to minimize the contradirectional coupling between the two waveguides, which will distort the measured spectrum. Secondly, as the grating continuously couples the optical power out along the length of the device, the detected interferogram is actually superimposed with an exponential decay. To optimize the SNR, the gap between the waveguides should be carefully chosen according to the grating strength to ensure a decay of  $1/e$  over the whole length of the interferogram we want to measure. Moreover, the grating should be positioned in the region where the evanescent field of the two waveguide modes has similar strength, so that we can capture the interferogram with the best contrast.

### 3. Bandwidth and resolution

The proposed co-propagative stationary FTS has a relatively broad operational bandwidth. Theoretically, the only limit is the lower wavelength boundary set by the Nyquist-Shannon sampling theorem, which tells us that to avoid subsampling, the smallest wavelength that can be sampled is  $\lambda_{min} = 2\Lambda\Delta n_{eff}$ , where  $\Lambda$  is the pixel pitch of the detector array. However, an upper boundary does exist due to both the losses of the  $Si_3N_4$  waveguide platform at longer wavelengths and the dispersive nature of the grating. Even under these considerations, our design can operate in the NIR region with a bandwidth over minimally 100 nm. The resolution of our FTS design is mainly limited by  $L$ , the length of the interferogram one can capture. Because of the finite length of the interferogram, the delta-shape spectrum in the Fourier domain for a single wavelength injection will be broadened into a sinc line shape,  $\sin(\pi f_z L)/(\pi f_z L)$ , where  $f_z$  is the spatial frequency, i.e.  $\Delta n_{eff}/\lambda$  in our case. We can then define the theoretically attainable resolution at wavelength  $\lambda$  as  $1.207\lambda^2/(\Delta n_{eff}L)$ , the FWHM of the sinc shape spectrum.

### 4. Fabrication and Characterization

The first realization of the co-propagative stationary FTS was fabricated in a CMOS pilot line in IMEC [3]. The  $Si_3N_4$  is deposited using Plasma-Enhanced Chemical Vapor Deposition (PECVD) on top of a 2200 nm silicon oxide layer which lays on the silicon substrate. The waveguides, gratings and other structures are then patterned by deep UV lithography. In Fig. 1(b), we show the Scanning Electron Microscope (SEM) view of a small part of the FTS structure. In this picture, we can see the two  $Si_3N_4$  rib waveguides with a different width and a grating between them. The waveguides have a thickness of 220 nm, with a shallow etch of 110 nm to define the rib and are cladded with top oxide. The grating between the two waveguides has a total length of 7300  $\mu m$  and a period of 640 nm, which allows the interferogram to be diffracted out of the chip at a near-vertical angle. With a width of about 0.01 mm and length of around 10 mm, the footprint of a single co-propagative stationary FTS is actually very small ( $\sim 0.1 \text{ mm}^2$ ). Such a small size offers the potential for integrating many spectrometers on a single chip. For example, for the purpose of hyperspectral imaging with high spectral resolution.

In the preliminary experimental demonstration, monochromatic light (FWHM=0.5 nm) generated by a 895 nm laser source is injected horizontally into our FTS structure. An imaging system consisting of a microscope objective and a CCD camera is employed both to provide the optical view for alignment and to capture the interferogram. Since the image system has a limited field of view of 913  $\mu m$  wide in one frame, we numerically stitch 8 frames to obtain the whole interferogram (Fig. 1(c)), which extends to about 7300  $\mu m$ . To display the interference pattern with more

details, we show a zoom-in in Fig. 1(d). As expected, a cosine distribution of intensity is observed with a period of about  $24 \mu\text{m}$ , which corresponds to the difference in the effective index of 0.0376 of the two waveguide modes that generate the interferogram.

In Fig. 2(a), the intensity profile of the interferogram extracted from the stitched images is plotted. As expected, one can observe an exponential decay of the interferogram. We then compute the Discrete Fourier Transform of the interferogram to recover the spectrum of the incoming light. The result of the Fourier Transform is then mapped onto the axis of wavelength as shown in Fig. 2(b). To match the position of the peak with our laser source wavelength, we use the difference in effective index  $\Delta n_{eff} = 0.0376$ , which is not far away from the simulation result of the index difference 0.0387.

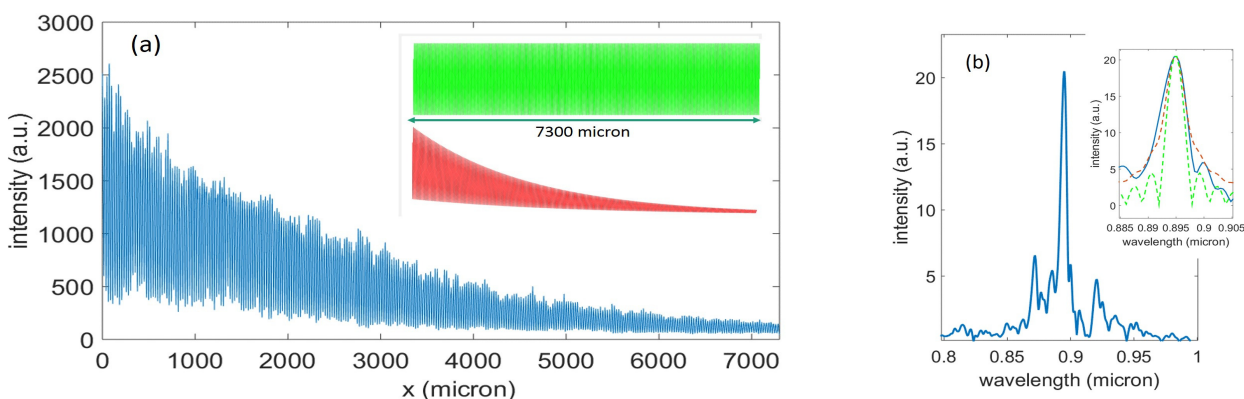


Fig. 2: (a) The intensity profile of the measured interferogram. The inset plots the computed standard (green) and modulated (red) cosine profile with same period and total length as the measured one. (b) the spectrum computed with measured interferogram. In the inset, the green and red spectra are computed with the green and red profiles in (a) respectively .

The FWHM of the spectrum is measured to be 6 nm, while the theoretical value should be 3.5 nm. To study the reasons of the broadening, we plot in the inset of Fig. 2(b) the green and red dash spectrum computed from a standard cosine profile and the one modulated by the same decay (the green and red profile in the inset of Fig. 2(a)). The green spectrum has a FWHM of 3.5 nm as we expected and the red one 5.5 nm. It is obvious that the spectrum is broadened mainly due to the superposition of the exponential decay. We attribute the small spectral features in the blue spectrum to small fabrication variations in the grating, distortion from the imaging system and to the fact that we are stitching 8 images. To fully understand and remove these features, further work is still required.

## 5. Conclusion

In this paper, we described a novel way to implement the integrated stationary FTS. For first prototyping, the proposed structure is fabricated on a  $\text{Si}_3\text{N}_4$  waveguide platform with CMOS compatible technologies. We also demonstrated and discussed the preliminary characterization results which are in agreement with the theoretical expectations. Although more work is necessary to characterize and improve the performance, we believe the proposed co-propagative stationary FTS is a promising choice for a robust on-chip spectrometer. While limited by the transparency window of the waveguide platform, this FTS can be designed for any wavelength between  $0.4\text{--}6.5 \mu\text{m}$ , which makes it a good candidate for further integration of many lab-on-a-chip systems (e.g., the on-chip Raman or absorption spectroscopic systems [5, 6]) or for space applications.

**Acknowledgment:** The authors acknowledge ERC-InSpectra Advanced Grant and EU H2020 PIX4life Project.

## References

1. Le Coarer, E., et al. *Wavelength-scale stationary-wave integrated Fourier-transform spectrometry*. Nature Photonics 1.8 (2007): 473–478.
2. Florjanczyk, M., et al. *Planar waveguide spatial heterodyne spectrometer*. Society of Photo-Optical Instrumentation Engineers (SPIE) Conference Series. Vol. 6796. 2007.
3. Subramanian, A. Z., et al. *Low-loss singlemode PECVD silicon nitride photonic wire waveguides for 532-900 nm wavelength window fabricated within a CMOS pilot line.*, IEEE Photonics Journal, 5(6), p.2202809 (2013)
4. Nie, X., et al. *Novel concept for a broadband co-propagative stationary Fourier Transform Spectrometer integrated on a  $\text{Si}_3\text{N}_4$  waveguide platform.*, CLEO: Applications and Technology. OSA, 2016.
5. Dhakal, A., et al. *Nanophotonic Lab-On-A-Chip Raman sensors: a sensitivity comparison with confocal Raman microscope.*, BioPhotonics 2015, Italy, p.Th6.3
6. Ryckeboer, E., et al. *Glucose sensing by waveguide-based absorption spectroscopy on a silicon chip*, Biomedical optics express, 5(5), p.1636-1648 (2014)